Drug-Induced p53 Activation Promotes Acinar Cell Identity and Prevents Pancreatic Cancer Initiation.

Jennifer J Twardowski [1,2], Thomas I Heist [1], Zamira Guerra Soares [1], Emily S Berry [1], Luis I Ruffolo [3], Christoph Pröschel[1], Stephano S Mello [1*]

1- Department of Biomedical Genetics, University of Rochester Medical Center, Rochester, NY 14642

2- Department of Biochemistry and Biophysics, University of Rochester Medical Center, Rochester, NY 14642

3- Department of Surgery, University of Rochester Medical Center, Rochester, NY 14642

*- Corresponding author: Stephano S. Mello

Email: stephano_mello@urmc.rochester.edu

Keywords:

Pancreatitis, ADM, p53, PanIN, plasticity, metaplasia, preneoplastic, acinar, Nutlin-3a, Mist1

Author Contributions: J.J.T. and S.S.M. were responsible for designing the study and preparing the manuscript. J.J.T. executed most of the experiments and analyzed the data. T.I.H. performed the embryonic studies and the ChIP-seq data analysis. Z.G.S. performed the CRISPRi assays and RT-qPCRs. E.S.B. assisted with figure preparation. L.I.R. was responsible for the initial whole-slide scans and histological analyses. C.P. assisted T.I.H. with embryo dissections. S.S.M. performed analysis of the RNA-seq data.

Competing Interest Statement: The authors declare no other competing financial interests.

Abstract

Pancreatitis is a painful inflammatory disease that carries an increased risk of developing pancreatic cancer. Patients with this disease experience acinar-to-ductal metaplasia (ADM), a process in which their pancreatic acinar cells dedifferentiate into a more ductal-like state. Metaplastic cells can proliferate and repopulate the pancreas before redifferentiating into functional acini. However, when metaplastic cells develop activating mutations in the oncogene Kras, they can progress into pancreatic intraepithelial neoplasias (PanINs). p53 has been recently shown to limit ADM, yet the underlying mechanisms of this function has not been explored in detail. Here, by treating mouse models of acute pancreatitis with Nutlin-3a (a non-genotoxic inducer of p53), we have found that mild p53 activation can significantly preserve functional acinar cells and restrain the formation of premalignant lesions. Our results also show that mild p53 activation can mitigate mutant Kras-prompted proliferation without adversely affecting the regeneration of acinar cells following pancreatitis. Leveraging a novel *in vivo* system to label metaplastic cells, we observe ADM redifferentiation into acini following treatment with Nutlin-3a, unequivocally establishing a new role of p53 in inducing ADM redifferentiation. Our data indicate that this role is mediated through the acinar transcription factor Mist1, which we highlight as a novel p53 target gene. Our findings also suggest that MDM2 inhibitors hold promise as a therapeutic approach for individuals at risk of developing pancreatic adenocarcinoma, including patients with pancreatitis.

Acknowledgements

The authors would like to thank Dr. Joshua Munger for providing immortalized MRC5 cells. We would also like to thank Jeffrey Fox and Vidya Venkatramani in the CMSR Histology Core for providing tissue processing and sectioning services. Lastly, we would like to thank Dr. Hartmut “Hucky” Land for his invaluable feedback throughout the creation of this work.

Introduction

Pancreatic ductal adenocarcinoma (PDAC) is a deadly disease which is currently the third leading cause of cancer deaths[1]. Activating mutations in the proto-oncogene Kras are nearly ubiquitous in PDAC, detectable in over 90% of cases, followed by TP53 mutations, which affect 78% of PDAC cases[2]. Other frequently mutated genes in PDAC include CDKN2A and SMAD4[3, 4]. The essential role of Kras mutations in the initiation and maintenance of PDAC has been established by several studies using genetically engineered mouse models[5-7]. On a cellular level, Kras mutations induce inflammation and de-differentiation of normal pancreatic cells, leading to acinar-to-ductal metaplasia (ADM), a process in which acinar cells lose their characteristic expression of Mist1 and Amylase and acquire ductal markers such as Sox9 and Cytokeratin-19[8-10]. Normally, ADM is a transient process that resolves within 4-10 days after a case of acute pancreatitis[9]. However, metaplastic cells become unable to re-differentiate if activating mutations in Kras (such as *Kras*^{G12D}) are present, and instead form preneoplastic pancreatic lesions known as pancreatic intraepithelial neoplasia (PanIN)[11]. Concerningly, PanIN lesions hold the potential to develop into PDAC.

Certain medical conditions, such as chronic and autoimmune pancreatitis, increase the risk of PDAC by causing Kras mutations in the pancreatobiliary regions, which affect up to 37% of patients[12, 13]. These mutations, in conjunction with the inflammatory environment which occurs during pancreatitis, put patients at an increased risk of developing PanIN and PDAC. As such, pancreatitis patients have a 6 times increased risk of developing PDAC when compared to the general population[14]. Elucidating the molecular mechanisms underlying acinar cell reprogramming and the formation of PanIN is essential for the development of new therapeutic approaches for pancreatitis.

While Kras mutations are observed early and thought to be driver mutations for PanIN formation, p53 mutations are typically found in more advanced PanIN, and were initially thought to promote the transition from PanIN to PDAC[15]. Specifically, earlier research has suggested that p53's role in suppressing the transition from PanIN to PDAC lies on its ability to induce senescence in preneoplastic lesions[16]. However, this model of p53 as a barrier for PanIN to PDAC progression is contradicted by evidence of p53 mutations at earlier stages, such as in ADM or early PanINs[15, 17-19]. The role of p53 in suppressing transformation and PDAC formation at earlier stages, as well as the underpinning molecular mechanisms behind this process are incompletely understood.

p53 triggers various cellular responses by activating the transcription of target genes[20]. Early studies suggested that p53-controlled acute DNA damage responses such as apoptosis and cell cycle arrest were the basis of p53-mediated tumor suppression[21]. However, experimental evidence from murine models has demonstrated that p53-dependent cell cycle arrest and apoptosis responses are not essential for tumor suppression[22-25], suggesting that p53 could be triggering additional tumor suppressive cellular responses. More recently, novel p53-controlled cellular responses with a potential role in tumor suppression have been identified. For instance, p53 has been found to influence ferroptosis, genomic integrity, metabolism, stemness, and immunity, all of which could contribute to tumor suppression[26-30]. Moreover, p53 signaling has been shown to suppress the expression of stem cell factors, indicating that p53 is not only a tumor suppressor, but also a promoter of differentiation[31-33]. Recent studies using a hyperactive p53 mouse model with key mutations in its second transactivation domain (*Trp53*^{F53Q,F54S}, also referred as *p53*^{53,54}) have demonstrated that p53 can induce differentiation of metaplastic cells and promote tissue regeneration in mouse models for pancreatic and lung

cancer harboring a mutant *Kras* allele, contributing to p53-mediated tumor suppression[34, 35]. In the pancreas specifically, it was shown that the *p53*^{53,54} allele induces the re-differentiation of metaplastic acini, thereby decreasing PanIN formation, pancreatic inflammation, and promoting pancreatic regeneration[34]. We previously hypothesized that *p53*^{53,54}'s hyperactivity could be related to its increased stability[36]. However, p53's transactivation domains are involved in recruiting transcriptional factors and chromatin modifiers to regulatory regions of p53-controlled genes[37], suggesting that the effect might stem from changes in p53's protein interactions rather than its enhanced stability. The exact mechanisms by which p53 controls acinar cell identity and differentiation in normal and disease contexts, as well as the therapeutic potential of the findings with the p53^{53,54} allele, remain unclear.

Here, we leverage an oncogenic Kras-driven PDAC model and drug-induced p53 stabilization to investigate the molecular mechanisms underlying p53-mediated acinar cell differentiation, as well as its therapeutic potential for diseases where Kras mutations may facilitate the formation of preneoplastic lesions and increase the risk of PDAC, such as pancreatitis. To explore drug-induced p53 activation as a possible treatment for the treatment of precancerous transformation, we treated mice harboring a mutant Kras allele with cerulein (a drug analogous to cholecystokinin) and Nutlin-3a, a cis-imidazole analog that stabilizes p53[38]. Our experiments provide evidence that mild p53 stabilization is sufficient to induce acinar cell differentiation, and that p53 participates in the transactivation of key genetic programs involved in acinar cell identity in both disease and developmental contexts.

Results

Mild p53 activation promotes pancreatic regeneration following pancreatitis

It was previously speculated that the p53 mutant carrying two amino acid alterations on the second p53 transactivation domain (*Trp53*^{F53Q,F54S}) was hyperactive due to its increased protein stability[36]. Alternatively, p53's transactivation domain may modulate the transcriptional activity of p53 target genes by interacting with other transcription factors or chromatin modulators[37]. To test if p53 stability promotes pancreatic regeneration, we induced pancreatitis in 2-month-old *Kras*$^{LSL\text{-}G12D/+}$*;Ptf1a-Cre* (*KC*) mice using the chemical irritant cerulein, and followed with daily intraperitoneal injections of the Mdm2 inhibitor Nutlin-3a or DMSO (mock) for one week (**Figure 1a**). A range of concentrations of Nutlin-3a (25, 12.5, 6, and 3 mg/kg of body weight) were used to treat the animals. We then investigated the impact of drug-induced p53 stabilization on the pancreas recovery from acute pancreatitis by quantifying p53 levels and acinar cell recovery.

We assessed overall pancreas histology by hematoxylin and eosin stain (H&E) and examined acinar recovery by immunohistochemistry for the acinar cell marker Amylase (**Figure 1b**). Interestingly, drug-induced p53 activation promotes recovery from ADM and regeneration of fully differentiated acini optimally at concentrations of 6 mg/kg of body weight of Nutlin-3a. This suggests that mild p53 activation reproduces the effects seen with the *p53*^{53,54} allele, but excessive p53 stabilization negatively impacts pancreas regeneration upon pancreatitis. In addition to the differences in Amylase, we also observed striking differences in pancreatic size between cohorts. Mock-treated *KC* mice had abnormally large pancreata, as previously observed[6], while Nutlin-3a-treated *KC* mice had smaller pancreata that were not significantly larger than those of *Kras*^{WT} mice (**Supplemental Figure 1a**). This data suggests that pancreatic regeneration through p53 activation does not

promote significant gains or losses in pancreatic size when compared to pancreatic regeneration in wild-type mice.

To verify that a similar initial level of damage was generated in both DMSO- and Nutlin-3a-treated cohorts, we sacrificed mice one and two days after induction of acute pancreatitis and evaluated Amylase levels as a surrogate for acinar cell loss. Amylase staining revealed similar levels of acinar cell loss in both DMSO- and Nutlin-3a-treated cohorts (**Supplemental Figure 1b**), suggesting that both groups of mice were effectively injured by cerulein-induced pancreatitis. To ensure that our results were an effect of Nutlin-3a-mediated p53 activation, and not the activation of other Mdm2 targets[39], we treated 2-month-old *Kras*$^{LSL\text{-}G12D/+}$;*p53*$^{fl/fl}$;*Ptf1a-Cre* (*KPC*) mice with cerulein and administered Nutlin-3a (6 mg/kg of body weight) for one week. *KPC* mice subjected to cerulein-induced acute pancreatitis exhibited significant loss of acinar tissue, which was not restored following treatment with Nutlin-3a (**Figure 1c**). Compared to the significant preservation of acinar tissue we observed in Nutlin-3a-treated *KC* mice, Nutlin-3a treatment had no significant effect on pancreatic regeneration in *KPC* mice, indicating that the expression of p53 is required for acinar regeneration.

To determine whether a dosage of 6mg/kg of body weight of Nutlin-3a effectively activates p53 in the pancreas, we next examined p53 activation by immunohistochemistry, and found p53 stabilization to be localized within ADM structures (**Figure 1d**). The selective localization of p53 in ADM structures suggests a differential regulatory mechanism of p53 in metaplastic cells. As expected, no p53 expression was observed in *KPC* mice. To further evaluate if p53 stabilization impacts cell cycle in cells that suffered ADM, we analyzed Ki67-positive ADM cells and found a significant reduction in Ki67-positive nuclei following treatment with Nutlin-3a only in *KC* mice, but not in *KPC* mice (**Supplemental Figure 1c**). These findings indicate that while Nutlin-3a-induced p53 stabilization counteracts the abnormal proliferation prompted by mutant Kras, it does not adversely affect the normal regenerative process of acinar cells following pancreatitis.

Mild p53 activation reduces the formation of PanIN during pancreatitis.

Patients suffering from pancreatitis have elevated levels of both PanIN and Kras mutations[12, 13]. These preneoplastic lesions arise from metaplastic acini with Kras mutations, as shown by mouse models[5, 6, 8, 10]. Therefore, mild p53 stabilization, which reduces ADM proliferation and preserves acinar structure, may serve as a preventative treatment for PanIN formation. To investigate the effects of drug-induced p53 activation on PanIN formation, we induced pancreatitis in *KC* mice using cerulein, followed by a daily treatment with either Nutlin-3a or DMSO (mock). PanIN lesions were identified using H&E, Alcian blue, and Mucin5ac, the latter of which are specific markers for PanIN[6, 40]. Alcian blue and Mucin5ac quantification in both Nutlin-3a- and mock-treated cohorts showed that Nutlin-3a-treated *KC* mice have a two-fold decrease in PanIN formation relative to mock-treated cohorts (**Figure 2a**), suggesting that drug-induced p53 activation can also reduce the formation of PanIN in mice with pancreatitis. *KPC* mice exhibited higher levels of both Alcian blue and Mucin5ac than their *KC* counterparts, and were not affected by treatment with Nutlin-3a.

p53 is known to limit cell cycle progression[41], an effect that could contribute to the decrease in PanIN lesions in Nutlin-3a-treated mice. To test if drug-induced p53 stabilization can interfere with PanIN expansion by limiting cell division, we counted double-positive cells for the PanIN marker Alcian blue and the cell proliferation marker Ki67. We found that *KC* mice treated with Nutlin-3a have approximately half the level of Ki67 expression in

PanIN as mock-treated *KC* mice (**Supplemental Figure 2a**). This effect was lost in *KPC* mice, which expressed high levels of Ki67 in PanIN regardless of treatment group.

To test if drug-induced p53 activation reduces Kras signaling, we used immunostaining to detect the Kras signaling marker phospho-ERK1/2 and measured ERK activation in Alcian blue-positive PanIN, in both Nutlin-3a- and mock-treated cohorts (**Figure 2b**). Our results show a decrease in phospho-ERK1/2 signaling in *KC* mice treated with Nutlin-3a, suggesting that drug-induced p53 stabilization can suppress Kras signaling in preneoplastic lesions. *KPC* mice showed high levels of phospho-ERK1/2 staining within PanIN, irrespective of treatment group. We also observed a markedly decreased pancreatic desmoplastic reaction in Nutlin-3a-treated *KC* mice, as evidenced by Trichrome staining (**Figure 2c**), a reaction that was previously connected to alterations in Kras signaling[5, 42]. Both treatment groups of *KPC* mice exhibited higher levels of fibrosis than both cohorts of *KC* mice. Taken together, these results show that drug-induced p53 stabilization prevents PanIN formation in part by limiting ADM, but also by inhibiting PanIN proliferation and Kras signaling.

p53 controls the expression of acinar cell identity genes

p53 is a transcription factor, capable of controlling the expression of target genes by binding to its regulatory elements[20]. To define the mechanisms behind p53's ability to promote the redifferentiation of metaplastic acinar cells, we used ChIP-seq data sets that were previously generated from mouse embryonic fibroblasts (MEFs) and primary human fibroblasts (MRC5) treated with doxorubicin[43, 44]. We also used a previously published RNA-seq data from sorted CD133-positive cells, comprised of ADM and precursor lesions, from the pancreas from *KC* and *KPC* mice at 6-8 and 4-6 weeks, respectively, as these ages show ADM and precursor lesions, but not cancer[36]. We used this data set together with the mouse and human p53 ChIP-seq data sets to define novel p53 target genes that could play a role in its ability to promote an acinar cell state. This analysis revealed a p53-binding peak conserved in both mice and humans at an essential gene involved in the control of acinar cell identity: the basic helix-loop-helix transcription factor *Bhlha15 (Mist1)* (**Figure 3a**).

To examine the p53-dependency of *Bhlha15* in the pancreas, we used previously published RNA-seq analysis on p53 proficient and deficient cells, as described above. Our results showed that the expression level of *Bhlha15* was significantly decreased in the absence of p53 in preneoplastic pancreatic cells (**Figure 3b**). To further validate if the expression of *Bhlha15* is dependent on p53 in other mouse cell types, we performed RT–qPCR analysis of wild-type and *p53*$^{-/-}$ MEFs treated with the DNA damaging agent doxorubicin, and found that the expression of *Bhlha15* is dependent on p53 (**Figure 3c**). Collectively, these findings suggest that p53 exerts regulatory control over the critical acinar cell identity gene *Bhlha15* across various mouse cell types and in different contexts. These data are consistent with a recent ATAC-seq study that suggests that p53 plays a role in promoting chromatin accessibility on genes involved in acinar cell identity[34].

We also tested if p53 regulation of *BHLHA15* is conserved in human cells. To establish the contribution of p53 in the expression of this gene in human cells, we used CRISPR interference (CRISPRi) to knockdown p53 in primary human fibroblasts, and treated these cells with doxorubicin. First, we confirmed p53 knockdown by qRT-PCR (**Supplemental Figure 3a**) and then tested the expression of *BHLHA15* in both untreated and doxorubicin-treated cells. Following the knockdown of p53 and DNA damage induced by doxorubicin, there was a marked

reduction in *BHLHA15* expression (**Figure 3d**). We propose that *BHLHA15* is a novel p53 target gene, and that it mediates p53's promotion of acinar identity.

To verify that *Bhlha15* was being activated by p53 in our Nutlin-3a-treated mice, we performed immunohistochemistry for its translated protein, Mist1, in pancreatic tissue samples. Mist1 was abundant in redifferentiated acini, as expected, but we also observed Mist1 expression in ADM regions of Nutlin-3a-treated *KC* mice, while no Mist1 staining was present in the ADM of mock-treated mice, indicating that the Mist1 expression was being driven by p53 activation (**Figure 3e**).

Although p53 knockout mice do not display overt symptoms of acinar hypoplasia, implying that p53 may not be critical for acinar cell development, our results prompt further investigation into the potential involvement of p53 in Bhlha15 activation during embryonic development. To that end, we extracted pancreata from wild-type mouse embryos at embryonic days 15.5 (E15.5) for subsequent histology and immunohistochemistry. Interestingly, p53 is stabilized specifically in proto-acinar cells at E15.5, alongside Mist1 and Amylase (**Supplemental Figure 3b**), suggesting that p53 might also play a role in acinar cell differentiation during embryonic development. Together, these findings suggest that p53 activation of *Bhlha15* is conserved in both mouse and human cells, supporting the idea that p53 plays an important role in defining the identity of pancreatic acinar cells.

p53 promotes the redifferentiation of metaplastic acinar cells

The classical p53 downstream effects are the regulation of cell cycle arrest and apoptosis in response to DNA damage, through the transactivation of key p53 target genes such as p21, Puma and Noxa[41, 46, 47]. However, we propose that p53 can trigger an acinar identity transcription program in the pancreas. Previous studies have investigated the role of p53 in cellular differentiation, linking it to the suppression of stemness factors in embryonic stem cells and the promotion of mesendodermal differentiation through the transactivation of Wnt signaling[48, 49]. To interrogate whether drug-induced p53 activation can promote the re-differentiation of metaplastic acini, we used an inducible *Sox9-Cre* allele and a *tdTomato* reporter gene silenced by a stop cassette flanked by loxP sites. As mentioned before, acini undergoing ADM gain a more ductal-like identity and start to express Sox9. By combining the inducible *Sox9-Cre* and the *tdTomato* alleles, we can label ADM cells with tdTomato and investigate the fate of metaplastic acini in Nutlin-3a-treated mice (**Figure 4a**).

To test this system in a pancreatic regeneration model, we first generated *Rosa26-CAG-LSL-tdTomato-WPRE;Sox9-Cre^{ER}* (*TS*) mice, induced acute pancreatitis using cerulein, and administrated tamoxifen to activate Cre recombinase concomitantly to ADM formation. After 1 week, we evaluated tdTomato positivity in the pancreas. As expected, all ductal cells were tdTomato-positive (**Figure 4b**). Our results showed that a small percentage of acinar cells were tdTomato-positive (**Figure 4c**), suggesting that this model could be used to investigate the re-differentiation of metaplastic acini. We also tested the inducible *Sox9-Cre* allele for leakiness, evaluating tdTomato positivity in mice without tamoxifen treatment, and did not observe any tdTomato-positive cells in either ductal or acinar compartments (**Supplementary Figure 4**).

To test the impact of Nutlin-3a treatment in acinar cell identity in a mutant Kras context, we induced pancreatitis in *Kras$^{LSL\text{-}G12D/+}$;Rosa26-CAG-LSL-tdTomato-WPRE;Sox9-Cre^{ER}* (*KTS*) mice, and administrated tamoxifen, as well as Nutlin-3a or DMSO (mock) for 1 week. Next, we extracted the pancreata of the mice and

performed a histological analysis of tdTomato-positive acini and ADM. We found that Nutlin-3a treatment increased the frequency of redifferentiated tdTomato-positive acini in *KTS* mice in comparison to mock-treated *KTS* mice (**Figure 4d**). Mock-treated *KTS* mice instead displayed tdTomato-positive regions of ADM, which were not present in Nutlin-3a-treated *KTS* mice. These results indicate that drug-induced p53 activation is promoting the redifferentiation of metaplastic acini. In summary, our ADM labeling experiments showed that drug-induced p53 activation can induce acinar redifferentiation in the context of $Kras^{G12D}$.

Discussion

Kras mutations, found in over 90% of PDAC cases[2], are a major driver of tumor initiation, triggering acinar-to-ductal metaplasia and subsequent PanIN formation[8]. Medical conditions such as chronic or autoimmune pancreatitis greatly elevate the risk of Kras mutations and the formation of PanIN lesions[12, 13]. Identifying mechanisms able to reverse mutant-Kras-induced metaplasia may enable early treatments that lower PDAC incidence in high-risk patients. Building on a recent study that showed that a mildly hyperactive p53 protein (*Trp53*^{F53Q,F54S} or *p53*^{53,54}) can induce the redifferentiation of metaplastic acini, decrease PanIN formation, and promote pancreatic regeneration in a mouse model for PDAC[34], here we explore the mechanisms and therapeutic potential of p53-mediated acinar cell differentiation. By treating mouse models of PDAC with the Mdm2 inhibitor Nutlin-3a, we established that mildly enhanced p53 stabilization significantly improves pancreatic regeneration following pancreatitis. These findings are in contrast with previous studies that suggest that increased p53 activity can lead to aging, compromised tissue renewal and tissue atrophy[50, 51]. Moreover, our observation that higher dosages of Nutlin-3a do not lead to pancreatic regeneration is in accordance with previous works, which suggest that over-activation of p53 can cause widespread apoptosis and aberrant gene expression[52]. Together, these findings demonstrate that different levels of p53 activation can lead to different responses in the pancreas, and that only mild p53 activation can trigger proper regeneration of acinar cells after pancreatitis.

Our studies also showed that mild p53 stabilization reduced ADM proliferation, overcoming the augmented proliferation which occurs due to mutant Kras. However, it did not impair overall pancreas regeneration, as Nutlin-3a treated mice had normal pancreatic size. The reduced proliferation of ADM also suggests that Nutlin-3a-induced p53 activation might hinder PanIN formation following pancreatitis. We tested this assumption and found that p53 activation helps to reduce the burden of PanIN lesions, supporting the idea that mild, drug-induced p53 stabilization upon pancreatitis decreases PanIN formation. We also observed a decrease in the proliferation of PanIN cells, which may contribute to a decreased expansion of PanIN lesions. To test the impact of p53 activation on Kras signaling, we examined phospho-ERK signaling in PanIN, and found that Nutlin-3a treatment reduced phospho-ERK levels. Microenvironmental alterations in the pancreas are linked to changes in Kras signaling and Kras mutation[5, 42], and we observed a markedly decreased pancreatic desmoplastic reaction and collagen deposition in Nutlin-3a treated mice. These alterations in desmoplastic reaction suggest that mild p53 activation can also induce non-cell autonomous responses. The interaction between p53 and Kras signaling has yet to be thoroughly explored, but previous research suggests that p53 activation can limit Kras signaling in the pancreas and in lung adenocarcinoma [34, 53]. We find that drug-induced p53 activation can also suppress Kras signaling in the pancreas.

The exact role of p53 in pancreatic regeneration after pancreatitis remains unclear. A recent ATAC-seq study of pancreatic cells from mice proficient or deficient for p53 showed that p53 enhances the accessibility of genes related to acinar cell identity[34]. Here, we further explore this question by examining how p53, as a transcription factor, supports acinar cell identity. We analyzed p53 ChIP-seq data sets in mouse and human cells and pancreas gene expression data in p53 proficient and deficient mice, and identified a novel p53 target gene relevant to acinar identity: the basic helix-loop-helix protein Bhlha15 (or Mist1), a key protein for acinar cell differentiation[54]. This newfound connection between p53 and acinar cell identity raises the question if p53 has a role in the normal development of the embryonic pancreas. Here, we show that p53 is activated during acinar cell differentiation at E15.5 together with Mist1, providing another line of evidence that Mist1 is a p53 target gene. Our analysis of previously published data along with confirmatory results in mouse and human cell lines suggests that *Bhlha15* is a *bona fide* p53 target gene.

A fundamental issue in this research is how p53's new role in pancreatic regeneration relates to its ability to re-differentiate acinar cells that have undergone ADM. To more closely study p53 in the context of ADM and acinar redifferentiation, we utilized a mouse model that labels ADM cells based on their expression of the ductal identity gene Sox9. These experiments revealed that Nutlin-3a treatment induced the redifferentiation of metaplastic acini harboring a $Kras^{G12D}$ mutation. A caveat of this model is that, due to the transitory nature of metaplasia, recombination in ADM cells is not as efficient as in ductal cells. Still, the model shows that Nutlin-3a-induced p53 activation promotes the redifferentiation of acini that have previously undergone ADM. Together, our findings support a novel connection between p53 and the acinar redifferentiation program, which can be pharmacologically induced after acute pancreatitis and ADM.

Here, we provide evidence that mild, drug-induced p53 activation can promote the redifferentiation of metaplastic acini in the presence of mutant Kras, and could potentially be used as a treatment strategy to limit pancreatic metaplasia and PDAC initiation. We also provide evidence that only mild p53 activation can promote acinar redifferentiation, while higher levels of p53 activation cause deleterious phenotypes that were previously associated with over-active p53 mutants[50, 51]. Additionally, we found that Mist1, a key factor for acinar cell differentiation, is a novel p53 target gene, bound and regulated by p53 in both mouse and human cells. Our results suggest that Mdm2 inhibitors may be suitable as a therapeutic strategy in patients at risk of developing PDAC, such as patients that suffer from pancreatitis. Testing whether interventions like the ones suggested in this paper could alter the fate of metaplastic cells and provide a protective effect against PDAC initiation will be essential for the development of therapeutic strategies using Mdm2 inhibitors as a preventative treatment against cancer.

Materials and Methods:

Animal Models

All animal experiments were previously approved and performed according to the University Committee on Animal Resources at the University of Rochester (UCAR). Mouse models for PDAC harboring a mutant Kras allele in the pancreas were generated by crossing $Kras^{LSL\text{-}G12D}$ mice[57] with *Ptf1a-Cre* mice[58]. Mouse models for PDAC without p53 were generated by crossing $p53^{fl/fl}$ mice[59] to $Kras^{LSL\text{-}G12D/+}$;*Ptf1a-Cre* (*KC*) mice. To label ADM

cells and investigate the fate of metaplastic acini, *Rosa26-CAG-LSL-tdTomato-WPRE* mice[60] were bred to *Sox9-Cre*^{ER} mice[61], allowing the induction of Tomato specifically in Sox9-positive cells. *LSL-tdTomato-WPRE;Sox9-Cre*^{ER} (*TS*) mice were further bred to *Kras*$^{LSL-G12D}$ mice. Induction of Sox9-Cre was performed by the treatment with tamoxifen (MP Biomedicals 156738) dissolved in corn oil and ethanol and administered via oral gavage once daily for three days as previously described[62].

To induce acute pancreatitis, 2-month-old mice were administered eight hourly intraperitoneal injections of 10 µg/mL cerulein (Bachem 4030451) in PBS over the course of two days, at a dosage of 100 µg/kg of body weight, as previously described[63]. For drug-induced p53 activation experiments, mice were given intraperitoneal injections of either Nutlin-3a (APExBIO A3671) diluted in DMSO or DMSO alone (mock treatment) once daily for one week, at dosages of 3 mg/kg, 6 mg/kg, 12.5 mg/kg, and 25 mg/kg.

Immunohistochemistry

After experimental treatments, mouse pancreata were extracted and stored in 10% formalin solution. Tissue samples were processed, paraffinized, and sectioned by the Wilmot Cancer Institute Histopathology Core and Histology, Biochemistry, and Molecular Imaging (HBMI) Core. Immunohistochemistry was performed on formalin-fixed, paraffin-embedded tissue sections according to a standard protocol. Primary antibodies included mouse monoclonal anti-AMYLASE (Santa Cruz Biotechnology sc-46657, 1:100), rabbit monoclonal anti-MIST1 (Cell Signaling Technology 14896T, 1:100), rabbit monoclonal anti-p-ERK1/2 (Cell Signaling Technology 4370S, 1:100), rabbit polyclonal anti-p53 (Invitrogen PA5-88098, 1:300), mouse monoclonal anti-KI67 (BD Pharmingen 550609, 1:100), and rabbit polyclonal anti-RFP (Rockland 600-401-379, 1:100). Secondary antibodies included biotinylated goat anti-rabbit (Vector Laboratories BA-1000, 1:200) and anti-mouse (Santa Cruz Biotechnologies sc-516142, 1:200) IgG antibodies, Alexa Fluor™ 555 goat anti-mouse (Invitrogen A28180, 1:200), and Alexa Fluor™ 647 donkey anti-rabbit (Invitrogen A-31573, 1:200) antibodies. Binding avidity for biotinylated antibodies was increased using the Vectastain ABC Kit (Vector Laboratories PK-4000). Binding of biotinylated antibodies was visualized using a DAB peroxidase substrate kit (Vector Laboratories SK-4100). Counterstains included Hematoxylin QS (Vector Laboratories H-3404), DAPI (eBioscience 00-4959-52), and Nuclear Fast Red solution (IHC World IW-3000B). Other stains included Alcian blue solution (IHC World IW-3000A), eosin, and Masson's trichrome (provided by HBMI Core).

Tissue Analysis

Stained tissue samples were scanned using an Olympus VS120 Virtual Slide Microscope and Scanner. Image analysis and quantification of IHC markers were performed using Visiopharm (v.2019.07; Hørsholm, Denmark) and QuPath[64]. For cytoplasmic staining, positively stained area was quantified and presented as a percentage of total pancreatic area. For nuclear staining, positively stained nuclei were counted and presented as a percentage of total nuclei. For nuclear quantification within metaplastic cells, ADM were manually set as regions of interest (ROI) based on morphology, and nuclei within the ROI were quantified. For nuclear quantification within PanIN lesions, lesions were set as ROI using Alcian blue positivity, and nuclei within the ROI were quantified. A Shapiro-Wilk test was used to evaluate distribution of the data. For normally distributed samples, an unpaired 2-tailed Student's T-test was performed. For data not normally distributed, a Kruskal-Wallis test was performed.

Significant outliers were excluded. Statistical tests were performed using RStudio. P-values less than 0.05 were considered statistically significant.

Sequencing Data and Analysis

p53 ChIP-seq data in mouse and human cells used for the identification of novel p53 target genes were previously published[43, 44] and obtained from Gene Expression Omnibus (GEO, GSE46240 and GSE55727 respectively). RNA-seq data from preneoplastic lesions sourced from p53 wild-type (*Kras*$^{LSL\text{-}G12D/+}$*;Pdx1-Cre*) and p53 knockout (*Kras*$^{LSL\text{-}G12D/+}$*;Pdx1-Cre;p53*$^{-/-}$) mice were also previously published[36] and obtained from GEO (GSE94566). ChIP-seq data was aligned to the mouse genome (mm10) or human genome (hg38) using Bowtie2[65]. Peaks were called using MACS2[66] and bigwig files for visualization of p53 ChIP-seq peaks were generated using deepTools[67]. ChIPseeker[68] was used to annotate p53 ChIP-seq peaks to genes. RNA-seq data was aligned using Salmon[69] and analyzed using DESEQ2[70]. Genes with a false discovery rate (FDR) of 0.1 or less were considered significant.

Cell Culture

Mouse embryonic fibroblasts (MEFs) were obtained from *p53*$^{fl/fl}$ mice and were infected with Ad5 CMV-Cre or Ad5 CMV-empty adenovirus to obtain p53 knockout and p53 wild-type cells. Telomerase-immortalized MRC5 cells were a kind gift from Dr. Joshua Munger[71]. Both cells were maintained in DMEM with 10% FBS. CRISPR interference (CRISPRi) was performed in MRC5 cells using a previously validated[72] guide RNA against p53 (GCCCTACGCCCAGCACCGGG) or a non-targeting scrambled guide (GCTGCATGGGGCGCGAATCA). Doxorubicin (Sigma) was used at 0.2 µg/mL to cause DNA damage and activate p53 in both mouse and human cells.

RT-qPCR analysis

For RT–qPCR, RNA was isolated using Trizol reagent (Invitrogen) and reverse-transcribed using High-Capacity cDNA Reverse Transcription Kit (Applied Biosystems) and random primers. PCR was performed in triplicate using PerfeCTa SYBR Green FastMix (Quantabio) and a QuantStudio 5 Real-Time PCR machine (Applied Biosystems), and the results were computed relative to a standard curve made with cDNA pooled from all samples. The average of three independent experiments were plotted and the primer sequences for RT–qPCR are listed in the **Supplemental Table 1**.

Appendix:

Figure 1: Mild p53 activation promotes pancreatic regeneration following pancreatitis. (A) Schematic of acute pancreatitis induction and treatment with Nutlin-3a or DMSO (mock). (B) (Left) Representative images of H&E and IHC staining for Amylase in pancreatic tissue from *Kras*$^{LSL\text{-}G12D/+}$*;Ptf1a-Cre* (*KC*) mice following cerulein-induced acute pancreatitis, and administration of varying doses of Nutlin-3a or DMSO (mock) (counterstain: hematoxylin). (Right) Quantification of Amylase (+) area as a percentage of total pancreatic area. n=6 mock-treated; n=3 to 4 Nutlin-3a-treated *KC* mice. (C) (Left) Representative Amylase IHC staining in *KC* and *Kras*$^{LSL\text{-}G12D/+}$*;p53*$^{fl/fl}$*;Ptf1a-Cre* (*KPC*) mouse pancreata following one week of treatment with either 6 mg/kg Nutlin-3a or DMSO (mock) (counterstain: hematoxylin). (Right) Quantification of Amylase (+) area as a percentage of total pancreas area. n=6 mock-treated *KC*; n=4 Nutlin-3a-treated *KC*, mock-treated *KPC*, and Nutlin-3a-treated *KPC* mice. (D) (Left) Representative images of IHC staining for p53 in *KC* and *KPC* mice (counterstain: hematoxylin). (Right) Quantification of p53(+) nuclei as a percentage of total nuclei. n=6 mock-treated *KC*; n=4 Nutlin-3a-treated *KC*; n=3 mock-treated and Nutlin-3a-treated *KPC* mice. Significance determined by unpaired two-tailed T test. (*): $p<0.05$; (**): $p<0.01$, (***): $p<0.001$.

Figure 2: Mild p53 activation reduces the formation of PanIN during pancreatitis. (A) (Left) Representative H&E, Alcian blue (counterstain: Nuclear Fast Red), and Mucin5ac (counterstain: hematoxylin) staining of pancreatic tissue stained from *KC* and *KPC* following cerulein-induced acute pancreatitis, and one week of treatment with 6 mg/kg Nutlin-3a or DMSO (mock). (Right) Quantification of Alcian blue(+) area and Mucin5ac(+) as a percentage of total pancreatic area. n=6 mock-treated *KC*; n=4 Nutlin-3a-treated *KC*, mock-treated *KPC*, and Nutlin-3a-treated *KPC* mice. (B) (Left) Representative images of IHC staining for pERK and Alcian blue in *KC* and *KPC* mice (counterstain: Nuclear Fast Red). (Right) Quantification of pERK(+) PanIN as a percentage of total selected PanIN. n=6 mock-treated *KC*; n=4 Nutlin-3a-treated *KC*; n=3 mock-treated and Nutlin-3a-treated *KPC* mice. (C) (Left) Representative images of Trichrome staining in *KC* and *KPC* mice. (Right) Quantification of fibrotic tissue as a percentage of total pancreatic area. n=6 mock-treated *KC*; n=4 Nutlin-3a-treated *KC*, mock-treated *KPC*, and Nutlin-3a-treated *KPC* mice. Significance determined by unpaired two-tailed T test. (*): $p<0.05$; (**): $p<0.01$, (***): $p<0.001$.

Figure 3: p53 controls the expression of acinar cell identity genes. (A) p53 ChIP-Seq peaks at *Bhlha15* in mouse and human fibroblasts. Numbers in parentheses indicate the numbers of base pairs in individual half-sites matching the consensus p53 response element sequence. Number between brackets indicate the space in nucleotides (nts) between the two half-sites. (B) RNA-seq data show p53-dependent expression of *Cdkn1a* as a control and of *Bhlha15*, proposed as a novel p53 target gene. (C) RT-qPCR analysis of *Cdkn1a* and *Bhlha15* in WT and p53-null MEFs treated with 0.2µg/mL doxorubicin (DOX) for 8 hours; normalized to GAPDH. (D) RT-qPCR analysis of *CDKN1A* and *BHLHA15* in human fibroblasts following CRISPRi-mediated p53 knockdown (sgTP53) and treatment with doxorubicin. sgScr: non-targeting scrambled guide. (E) (Left) Representative images of IHC staining for Mist1 in *KC* mice (counterstain: hematoxylin). (Right) Quantification of Mist1(+) nuclei within ADM. n=6 mock-treated *KC*; n=4 Nutlin-3a-treated *KC* mice. Significance determined by unpaired two-tailed T test. (*): $p<0.05$; (**): $p<0.01$.

Figure 4: p53 promotes the redifferentiation of metaplastic acinar cells. (A) Schematic of acute pancreatitis induction, administration of tamoxifen, and treatment with Nutlin-3a or DMSO (mock), with predicted outcomes of tdTomato-labeled ADM and/or acini. (B) Examples of tdTomato(+) ducts in *Rosa26-CAG-LSL-tdTomato-WPRE;Sox9-Cre*^{ER} (*TS*) mice, as indicated by H&E staining, IHC for tdTomato (counterstain: hematoxylin), and IF for RFP and Amylase (counterstain: DAPI). (C) Examples of tdTomato(+) acini in *TS* mice, as indicated by H&E staining, IHC for tdTomato (counterstain: hematoxylin), and IF for RFP and Amylase (counterstain: DAPI). (D) (Left) Examples of tdTomato(+) ADM in mock-treated *Kras*$^{LSL\text{-}G12D/+}$*;Rosa26-CAG-LSL-tdTomato-WPRE;Sox9-Cre*^{ER} (*KTS*) mice and tdTomato(+) acini in *KTS* mice treated with Nutlin-3a. (Right) Quantification of tdTomato(+) acini as a ratio of total tdTomato(+) non-ductal cells in *TS* and *KTS* mice. n=3. (E) Proposed model for p53-based acinar differentiation. Significance determined by unpaired two-tailed T test. (**): $p<0.01$.

Supplemental Figure 1: (A) (Left) Representative images of H&E-stained pancreata from *Kras*^{WT}, Nutlin-3a-treated *KC*, and mock-treated *KC* mice. (Right) Quantification of pancreatic area. (B) Representative images of IHC staining for Amylase in Nutlin-3a-treated and mock-treated *KC* mice one and two days after induction of acute pancreatitis (counterstain: hematoxylin). (C) (Left) Representative images of IHC staining for Ki67 in *KC* and *KPC* mice (counterstain: hematoxylin). (Right) Quantification of Ki67(+) nuclei within ADM. n=6 mock-treated *KC*; n=4 Nutlin-3a-treated *KC*, mock-treated *KPC*, and Nutlin-3a-treated *KPC* mice. Significance determined by unpaired two-tailed T test. (*): $p<0.05$; (**): $p<0.01$.

Supplemental Figure 2: (A) (Left) Representative images of IHC staining for Ki67 in *KC* and *KPC* mice (counterstains: Alcian blue and Nuclear Fast Red). (Right) Quantification of Ki67(+) nuclei within selected PanIN. n=6 mock-treated *KC*; n=4 Nutlin-3a-treated *KC*, mock-treated *KPC*, and Nutlin-3a-treated *KPC* mice.

Supplemental Figure 3: (A) Verification of CRISPRi knockdown of p53. (B) Representative images of IHC staining for p53, Mist1, and Amylase in embryonic mouse pancreatic tissue (counterstain: hematoxylin).

Supplemental Figure 4: (A) Representative images of *TS* and *KTS* mouse pancreata after cerulein-induced pancreatitis, but no treatment of tamoxifen. Examples of ducts and acini are shown.

Supplemental Table 1: Sequences of primers used in qPCRs.

References:

1. Oncology ASoC. Pancreatic Cancer - Statistics, 2022.
2. Bailey P, Chang DK, Nones K, et al. Genomic analyses identify molecular subtypes of pancreatic cancer. Nature 2016;531:47-52.
3. Caldas C, Hahn SA, da Costa LT, et al. Frequent somatic mutations and homozygous deletions of the p16 (MTS1) gene in pancreatic adenocarcinoma. Nat Genet 1994;8:27-32.
4. Wilentz RE, Iacobuzio-Donahue CA, Argani P, et al. Loss of expression of Dpc4 in pancreatic intraepithelial neoplasia: evidence that DPC4 inactivation occurs late in neoplastic progression. Cancer Res 2000;60:2002-6.
5. Collins MA, Bednar F, Zhang Y, et al. Oncogenic Kras is required for both the initiation and maintenance of pancreatic cancer in mice. The Journal of clinical investigation 2012;122:639-653.
6. Hingorani SR, Petricoin EF, Maitra A, et al. Preinvasive and invasive ductal pancreatic cancer and its early detection in the mouse. Cancer Cell 2003;4:437-50.
7. Ying H, Kimmelman AC, Lyssiotis CA, et al. Oncogenic Kras maintains pancreatic tumors through regulation of anabolic glucose metabolism. Cell 2012;149:656-70.
8. Habbe N, Shi G, Meguid RA, et al. Spontaneous induction of murine pancreatic intraepithelial neoplasia (mPanIN) by acinar cell targeting of oncogenic Kras in adult mice. Proc Natl Acad Sci U S A 2008;105:18913-8.
9. Karki A, Humphrey SE, Steele RE, et al. Silencing Mist1 Gene Expression Is Essential for Recovery from Acute Pancreatitis. PLoS One 2015;10:e0145724.
10. Zhu L, Shi G, Schmidt CM, et al. Acinar cells contribute to the molecular heterogeneity of pancreatic intraepithelial neoplasia. Am J Pathol 2007;171:263-73.
11. Ma Z, Lytle NK, Chen B, et al. Single-Cell Transcriptomics Reveals a Conserved Metaplasia Program in Pancreatic Injury. Gastroenterology 2022;162:604-620 e20.
12. Kamisawa T, Tsuruta K, Okamoto A, et al. Frequent and significant K-ras mutation in the pancreas, the bile duct, and the gallbladder in autoimmune pancreatitis. Pancreas 2009;38:890-5.
13. Furuya N, Kawa S, Akamatsu T, et al. Long-term follow-up of patients with chronic pancreatitis and K-ras gene mutation detected in pancreatic juice. Gastroenterology 1997;113:593-8.
14. Kirkegard J, Cronin-Fenton D, Heide-Jorgensen U, et al. Acute Pancreatitis and Pancreatic Cancer Risk: A Nationwide Matched-Cohort Study in Denmark. Gastroenterology 2018;154:1729-1736.
15. Lüttges J, Galehdari H, Bröcker V, et al. Allelic Loss Is Often the First Hit in the Biallelic Inactivation of the p53 and DPC4 Genes During Pancreatic Carcinogenesis. The American Journal of Pathology 2001;158:1677-1683.
16. Morton JP, Timpson P, Karim SA, et al. Mutant p53 drives metastasis and overcomes growth arrest/senescence in pancreatic cancer. Proceedings of the National Academy of Sciences 2010;107:246-251.
17. Baumgart M, Werther M, Bockholt A, et al. Genomic instability at both the base pair level and the chromosomal level is detectable in earliest PanIN lesions in tissues of chronic pancreatitis. Pancreas 2010;39:1093-103.
18. Heinmoller E, Dietmaier W, Zirngibl H, et al. Molecular analysis of microdissected tumors and preneoplastic intraductal lesions in pancreatic carcinoma. Am J Pathol 2000;157:83-92.
19. Gansauge S, Schmid RM, Muller J, et al. Genetic alterations in chronic pancreatitis: evidence for early occurrence of p53 but not K-ras mutations. Br J Surg 1998;85:337-40.
20. Unger T, Nau MM, Segal S, et al. p53: a transdominant regulator of transcription whose function is ablated by mutations occurring in human cancer. EMBO J 1992;11:1383-90.
21. Ventura A, Kirsch DG, McLaughlin ME, et al. Restoration of p53 function leads to tumour regression in vivo. Nature 2007;445:661-5.
22. Valente LJ, Grabow S, Vandenberg CJ, et al. Combined loss of PUMA and p21 accelerates c-MYC-driven lymphoma development considerably less than loss of one allele of p53. Oncogene 2016;35:3866-71.

23. Valente Liz J, Gray Daniel HD, Michalak Ewa M, et al. p53 Efficiently Suppresses Tumor Development in the Complete Absence of Its Cell-Cycle Inhibitory and Proapoptotic Effectors p21, Puma, and Noxa. Cell Reports 2013;3:1339-1345.
24. Brady CA, Jiang D, Mello SS, et al. Distinct p53 Transcriptional Programs Dictate Acute DNA-Damage Responses and Tumor Suppression. Cell 2011;145:571-583.
25. Li T, Kon N, Jiang L, et al. Tumor Suppression in the Absence of p53-Mediated Cell-Cycle Arrest, Apoptosis, and Senescence. Cell 2012;149:1269-1283.
26. Tarangelo A, Magtanong L, Bieging-Rolett KT, et al. p53 Suppresses Metabolic Stress-Induced Ferroptosis in Cancer Cells. Cell Reports 2018;22:569-575.
27. Klusmann I, Rodewald S, Müller L, et al. p53 Activity Results in DNA Replication Fork Processivity. Cell Reports 2016;17:1845-1857.
28. Kruiswijk F, Labuschagne CF, Vousden KH. p53 in survival, death and metabolic health: a lifeguard with a licence to kill. Nat Rev Mol Cell Biol 2015;16:393-405.
29. Krizhanovsky V, Lowe SW. Stem cells: The promises and perils of p53. Nature 2009;460:1085-1086.
30. Lujambio A, Akkari L, Simon J, et al. Non-cell-autonomous tumor suppression by p53. Cell 2013;153:449-60.
31. Akdemir KC, Jain AK, Allton K, et al. Genome-wide profiling reveals stimulus-specific functions of p53 during differentiation and DNA damage of human embryonic stem cells. Nucleic Acids Res 2014;42:205-23.
32. Choi YJ, Lin C-P, Ho JJ, et al. miR-34 miRNAs provide a barrier for somatic cell reprogramming. Nat Cell Biol 2011;13:1353-1360.
33. Mizuno H, Spike BT, Wahl GM, et al. Inactivation of p53 in breast cancers correlates with stem cell transcriptional signatures. Proc Natl Acad Sci U S A 2010;107:22745-50.
34. Mello SS, Flowers BM, Mazur PK, et al. Multifaceted role for p53 in pancreatic cancer suppression. Proceedings of the National Academy of Sciences 2023;120:e2211937120.
35. Kaiser AM, Gatto A, Hanson KJ, et al. p53 governs an AT1 differentiation programme in lung cancer suppression. Nature 2023.
36. Mello SS, Valente LJ, Raj N, et al. A p53 Super-tumor Suppressor Reveals a Tumor Suppressive p53-Ptpn14-Yap Axis in Pancreatic Cancer. Cancer Cell 2017;32:460-473.e6.
37. Raj N, Attardi LD. The Transactivation Domains of the p53 Protein. Cold Spring Harb Perspect Med 2017;7.
38. Vassilev LT, Vu BT, Graves B, et al. In vivo activation of the p53 pathway by small-molecule antagonists of MDM2. Science 2004;303:844-8.
39. Johnson J, Lagowski J, Lawson S, et al. p73 expression modulates p63 and Mdm2 protein presence in complex with p53 family-specific DNA target sequence in squamous cell carcinogenesis. Oncogene 2008;27:2780-7.
40. Kim GE, Bae HI, Park HU, et al. Aberrant expression of MUC5AC and MUC6 gastric mucins and sialyl Tn antigen in intraepithelial neoplasms of the pancreas. Gastroenterology 2002;123:1052-60.
41. el-Deiry WS, Tokino T, Velculescu VE, et al. WAF1, a potential mediator of p53 tumor suppression. Cell 1993;75:817-25.
42. Velez-Delgado A, Donahue KL, Brown KL, et al. Extrinsic KRAS Signaling Shapes the Pancreatic Microenvironment Through Fibroblast Reprogramming. Cellular and Molecular Gastroenterology and Hepatology 2022;13:1673-1699.
43. Kenzelmann Broz D, Mello SS, Bieging KT, et al. Global genomic profiling reveals an extensive p53-regulated autophagy program contributing to key p53 responses. Genes & Development 2013;27:1016-1031.
44. Younger ST, Kenzelmann-Broz D, Jung H, et al. Integrative genomic analysis reveals widespread enhancer regulation by p53 in response to DNA damage. Nucleic Acids Res 2015;43:4447-62.
45. Jaiswal SK, Raj S, DePamphilis ML. Developmental Acquisition of p53 Functions. Genes 2021;12:1675.

46. Nakano K, Vousden KH. PUMA, a novel proapoptotic gene, is induced by p53. Mol Cell 2001;7:683-94.
47. Oda E, Ohki R, Murasawa H, et al. Noxa, a BH3-only member of the Bcl-2 family and candidate mediator of p53-induced apoptosis. Science 2000;288:1053-8.
48. Akdemir KC, Jain AK, Allton K, et al. Genome-wide profiling reveals stimulus-specific functions of p53 during differentiation and DNA damage of human embryonic stem cells. Nucleic Acids Research 2013;42:205-223.
49. Wang Q, Zou Y, Nowotschin S, et al. The p53 Family Coordinates Wnt and Nodal Inputs in Mesendodermal Differentiation of Embryonic Stem Cells. Cell Stem Cell 2017;20:70-86.
50. Rodier F, Campisi J, Bhaumik D. Two faces of p53: aging and tumor suppression. Nucleic Acids Research 2007;35:7475-7484.
51. Papazoglu C, Mills A. p53: at the crossroad between cancer and ageing. The Journal of Pathology 2007;211:124-133.
52. Van Nostrand JL, Brady CA, Jung H, et al. Inappropriate p53 activation during development induces features of CHARGE syndrome. Nature 2014;514:228-32.
53. Feldser DM, Kostova KK, Winslow MM, et al. Stage-specific sensitivity to p53 restoration during lung cancer progression. Nature 2010;468:572-5.
54. Johnson CL, Kowalik AS, Rajakumar N, et al. Mist1 is necessary for the establishment of granule organization in serous exocrine cells of the gastrointestinal tract. Mech Dev 2004;121:261-72.
55. Ray-Coquard I, Blay JY, Italiano A, et al. Effect of the MDM2 antagonist RG7112 on the P53 pathway in patients with MDM2-amplified, well-differentiated or dedifferentiated liposarcoma: an exploratory proof-of-mechanism study. Lancet Oncol 2012;13:1133-40.
56. Andreeff M, Kelly KR, Yee K, et al. Results of the Phase 1 Trial of RG7112, a Small-molecule MDM2 Antagonist in Leukemia. Clin Cancer Res 2017;22:868-876.
57. Jackson EL, Willis N, Mercer K, et al. Analysis of lung tumor initiation and progression using conditional expression of oncogenic K-ras. Genes Dev 2001;15:3243-8.
58. Nakhai H, Sel S, Favor J, et al. Ptf1a is essential for the differentiation of GABAergic and glycinergic amacrine cells and horizontal cells in the mouse retina. Development 2007;134:1151-60.
59. Marino S, Vooijs M, van Der Gulden H, et al. Induction of medulloblastomas in p53-null mutant mice by somatic inactivation of Rb in the external granular layer cells of the cerebellum. Genes Dev 2000;14:994-1004.
60. Madisen L, Zwingman TA, Sunkin SM, et al. A robust and high-throughput Cre reporting and characterization system for the whole mouse brain. Nat Neurosci 2010;13:133-40.
61. Xu Z, Wang W, Jiang K, et al. Embryonic attenuated Wnt/beta-catenin signaling defines niche location and long-term stem cell fate in hair follicle. Elife 2015;4:e10567.
62. Flowers BM, Xu H, Mulligan AS, et al. Cell of Origin Influences Pancreatic Cancer Subtype. Cancer Discov 2021;11:660-677.
63. Jensen JN, Cameron E, Garay MV, et al. Recapitulation of elements of embryonic development in adult mouse pancreatic regeneration. Gastroenterology 2005;128:728-41.
64. Bankhead P, Loughrey MB, Fernandez JA, et al. QuPath: Open source software for digital pathology image analysis. Sci Rep 2017;7:16878.
65. Langmead B, Salzberg SL. Fast gapped-read alignment with Bowtie 2. Nat Meth 2012;9:357-359.
66. Gaspar JM. Improved peak-calling with MACS2. bioRxiv 2018:496521.
67. Ramírez F, Ryan DP, Grüning B, et al. deepTools2: a next generation web server for deep-sequencing data analysis. Nucleic Acids Research 2016;44:W160-W165.
68. Wang Q, Li M, Wu T, et al. Exploring Epigenomic Datasets by ChIPseeker. Current Protocols 2022;2:e585.
69. Patro R, Duggal G, Love MI, et al. Salmon provides fast and bias-aware quantification of transcript expression. Nature Methods 2017;14:417-419.
70. Love MI, Huber W, Anders S. Moderated estimation of fold change and dispersion for RNA-seq data with DESeq2. Genome Biol 2014;15:550.

71. Monaghan M, Munger J. Contributions of the Human Cytomegalovirus U(L)30-Associated Open Reading Frames to Infection. J Virol 2021;95.
72. Horlbeck MA, Gilbert LA, Villalta JE, et al. Compact and highly active next-generation libraries for CRISPR-mediated gene repression and activation. eLife 2016;5:e19760.

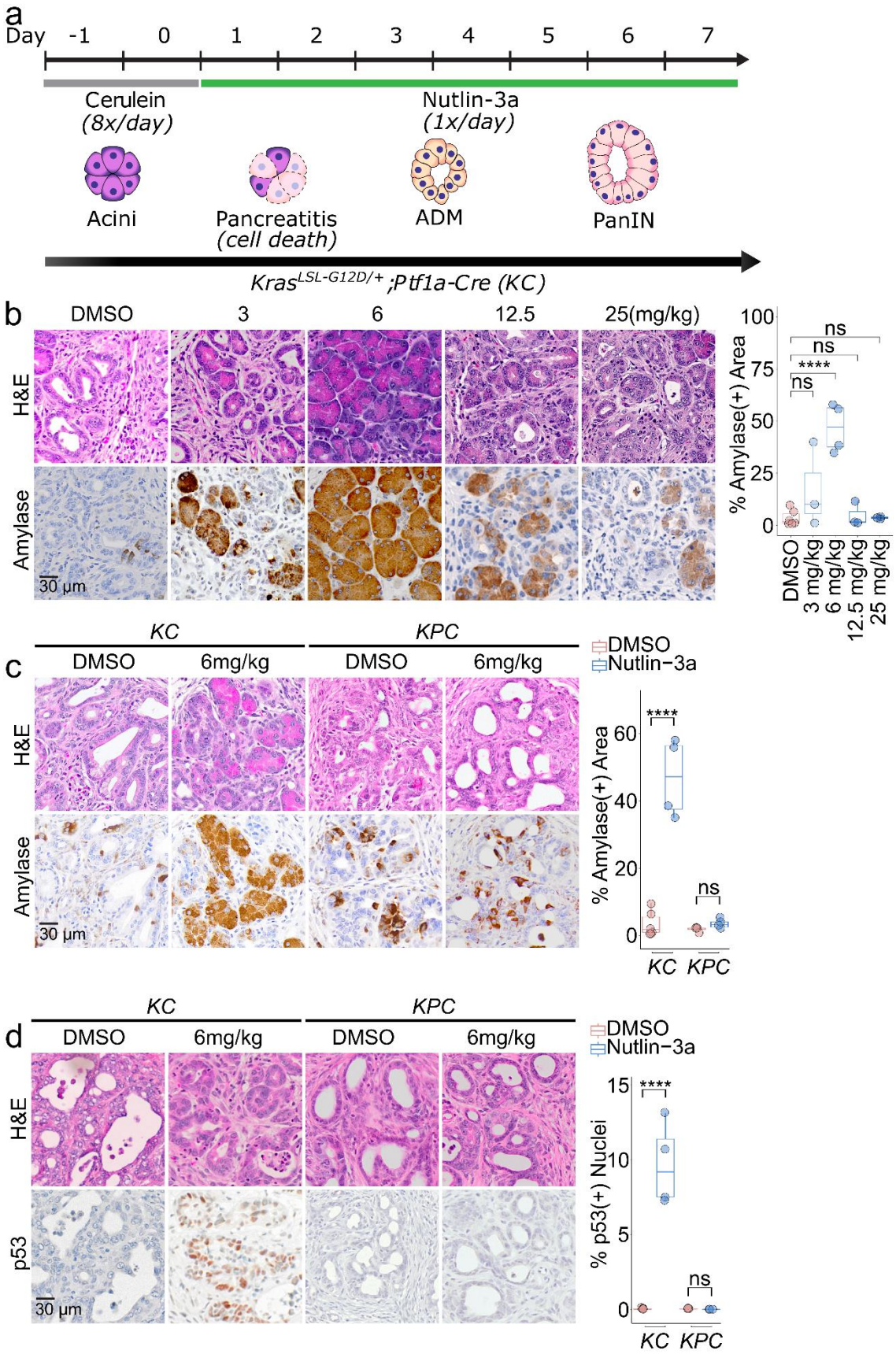
a
Day -1 0 1 2 3 4 5 6 7
Cerulein (8x/day)
Nutlin-3a (1x/day)
Acini
Pancreatitis (cell death)
ADM
PanIN
Kras LSL-G12D/+ ;Ptf1a-Cre (KC)
b
DMSO 3 6 12.5 25(mg/kg)
H&E
Amylase
30 µm
% Amylase(+) Area
ns
ns
****
ns
DMSO
3 mg/kg
6 mg/kg
12.5 mg/kg
25 mg/kg
c
KC
KPC
DMSO 6mg/kg DMSO 6mg/kg
DMSO
Nutlin−3a
H&E
Amylase
30 µm
% Amylase(+) Area
****
ns
KC KPC
d
KC
KPC
DMSO 6mg/kg DMSO 6mg/kg
DMSO
Nutlin−3a
H&E
p53
30 µm
% p53(+) Nuclei
****
ns
KC KPC

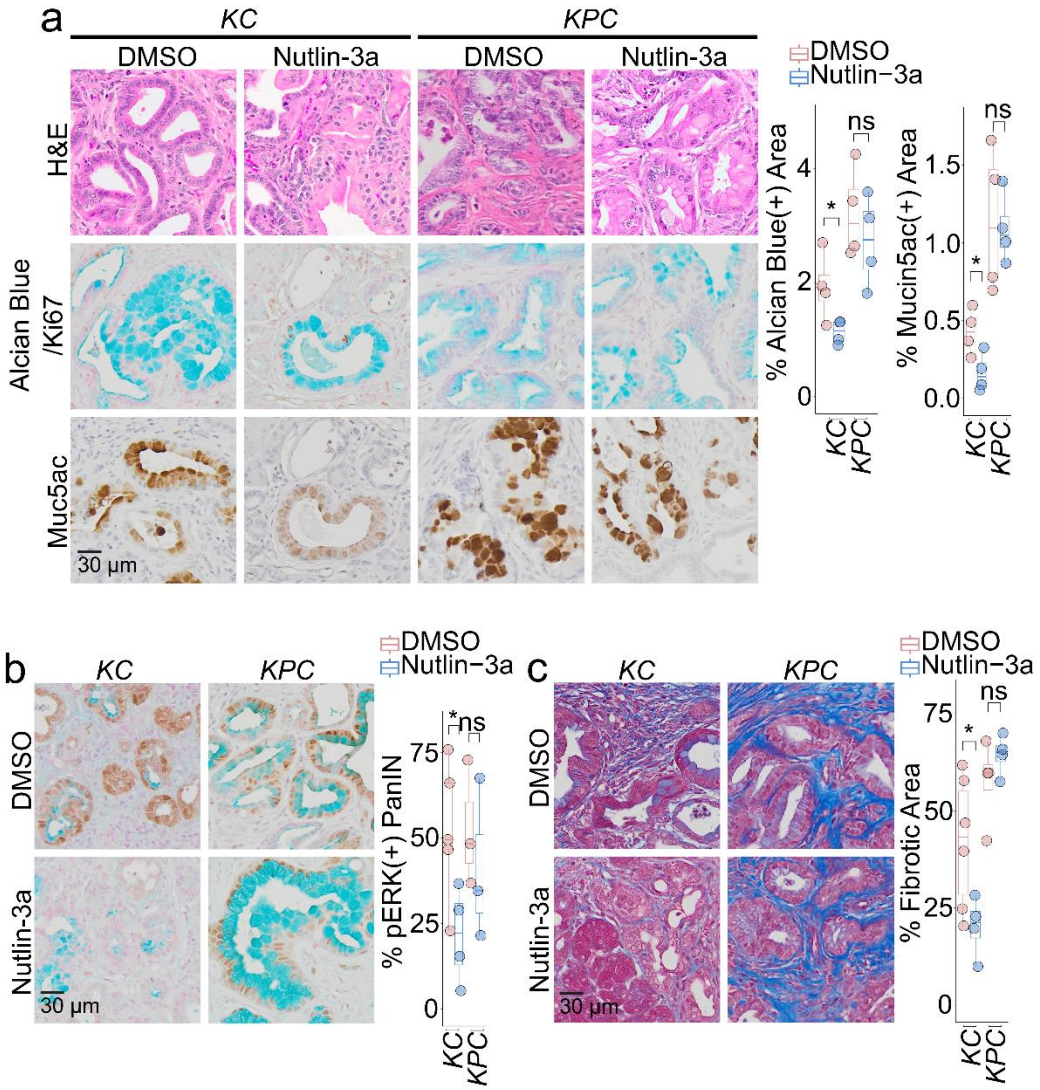
a
KC
KPC
DMSO
Nutlin-3a
DMSO
Nutlin-3a
H&E
Alcian Blue /Ki67
Muc5ac
30 µm
DMSO
Nutlin−3a
% Alcian Blue(+) Area
% Mucin5ac(+) Area
ns
*
KC
KPC
b
KC
KPC
DMSO
Nutlin-3a
30 µm
% pERK(+) PanIN
c
% Fibrotic Area

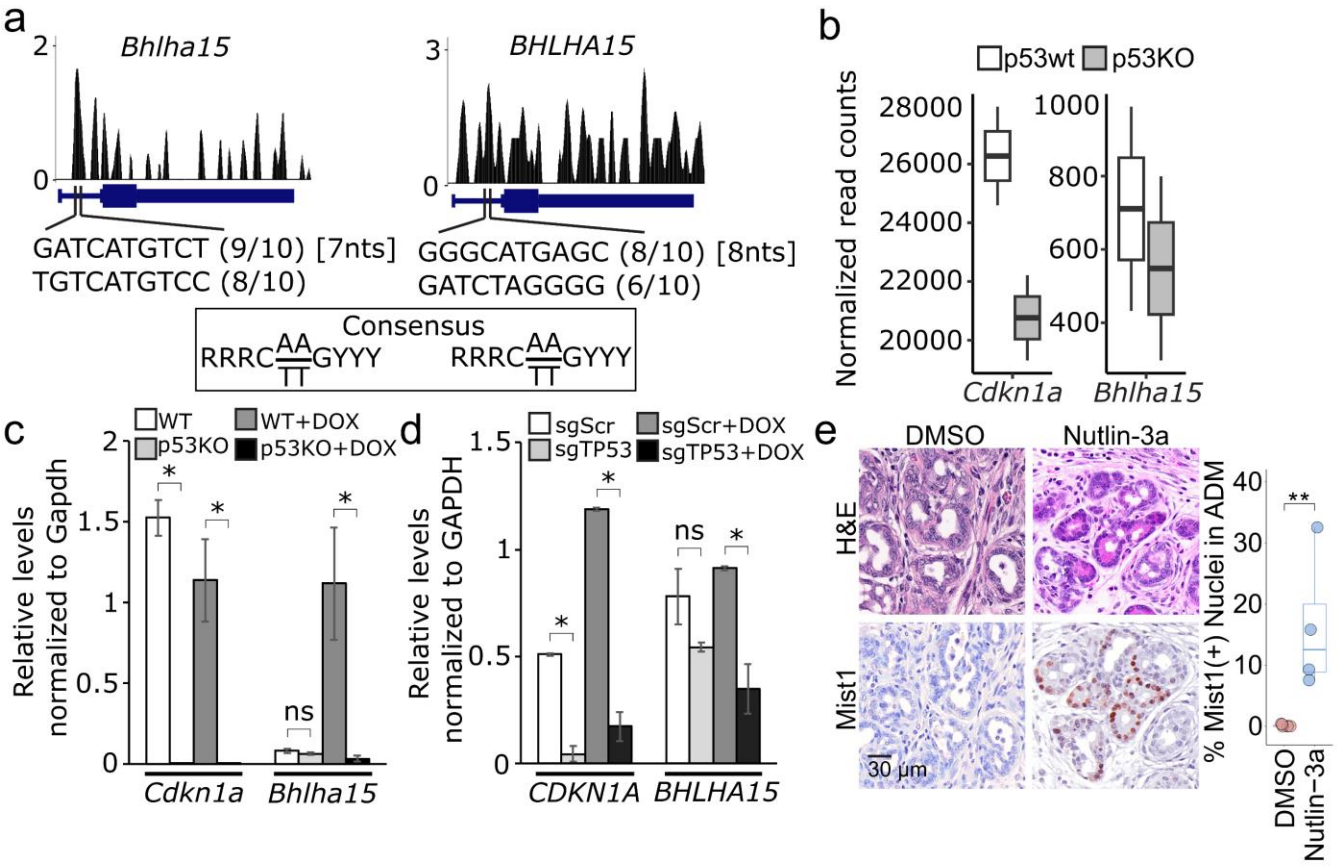
a
Bhlha15
BHLHA15
GATCATGTCT (9/10) [7nts]
TGTCATGTCC (8/10)
GGGCATGAGC (8/10) [8nts]
GATCTAGGGG (6/10)
Consensus
RRRCAAGYYY
RRRCAAGYYY
TT
TT
b
p53wt
p53KO
Normalized read counts
Cdkn1a
Bhlha15
c
WT
p53KO
WT+DOX
p53KO+DOX
Relative levels normalized to Gapdh
ns
Cdkn1a
Bhlha15
d
sgScr
sgTP53
sgScr+DOX
sgTP53+DOX
Relative levels normalized to GAPDH
ns
CDKN1A
BHLHA15
e
DMSO
Nutlin-3a
H&E
Mist1
30 µm
% Mist1(+) Nuclei in ADM
DMSO
Nutlin−3a

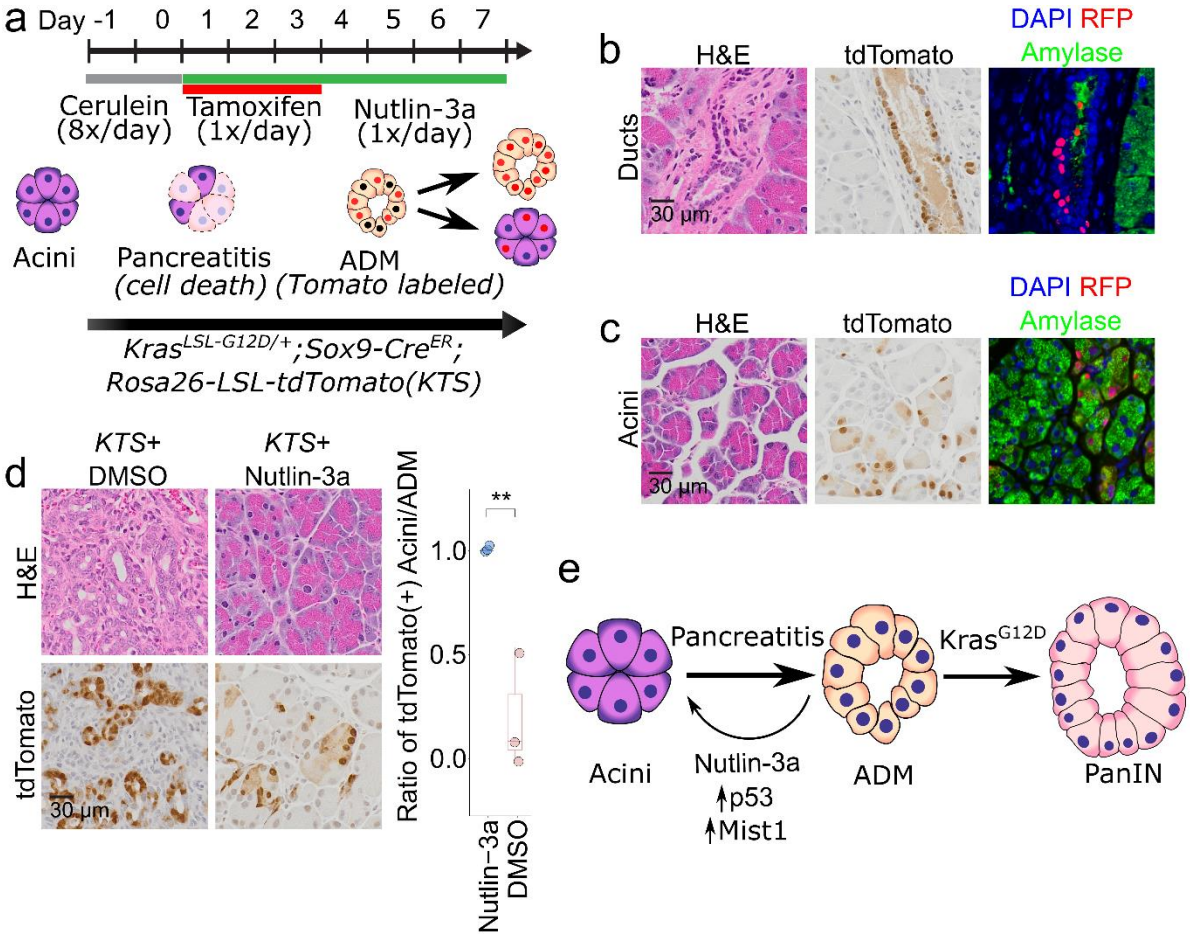
a
Day -1 0 1 2 3 4 5 6 7
Cerulein (8x/day)
Tamoxifen (1x/day)
Nutlin-3a (1x/day)
Acini
Pancreatitis (cell death)
ADM (Tomato labeled)
Kras^LSL-G12D/+;Sox9-Cre^ER; Rosa26-LSL-tdTomato(KTS)
b
H&E
tdTomato
DAPI RFP Amylase
Ducts
30 µm
c
H&E
tdTomato
DAPI RFP Amylase
Acini
30 µm
d
KTS+ DMSO
KTS+ Nutlin-3a
H&E
tdTomato
30 µm
Ratio of tdTomato(+) Acini/ADM
1.0
0.5
0.0
**
Nutlin-3a
DMSO
e
Acini
Pancreatitis
Nutlin-3a
↑p53
↑Mist1
ADM
KrasG12D
PanIN